Chinese Journal of Physics 68 (2020) 605–617

Contents lists available at ScienceDirect

Chinese Journal of Physics

journal homepage: www.sciencedirect.com/journal/chinese-journal-of-physics

A novel implementation of Petrov-Galerkin method to shallow water solitary wave pattern and superperiodic traveling wave and its multistability: Generalized Korteweg-de Vries equation

Seydi Battal Gazi Karakoc [*,a], Asit Saha [b], Derya Sucu [a]

[a] Department of Mathematics, Faculty of Science and Art, Nevsehir Haci Bektas Veli University, Nevsehir, 50300, Turkey
[b] Department of Mathematics, Sikkim Manipal Institute of Technology, Sikkim Manipal University, Majitar, Rangpo, East-Sikkim 737136, India

ARTICLE INFO

Keywords:
Finite element method
Petrov-Galerkin
Cubic B-spline
Soliton
Supernonlinear wave
Coexisting orbits

MSC:
65N30
65D07
74S05
74J35
76B25

ABSTRACT

This work deals with the constitute of numerical solutions of the generalized Korteweg-de Vries (GKdV) equation with Petrov-Galerkin finite element approach utilising a cubic B-spline function as the trial function and a quadratic function as the test function. Accurateness and effectiveness of the submitted methods are shown by employing propagation of single solitary wave. The L_2, L_∞error norms and I_1, $I_2$and I_3invariants are used to validate the applicability and durability of our numerical algorithm. Implementing the Von-Neumann theory, it is manifested that the suggested method is marginally stable. Furthermore, supernonlinear traveling wave solution of the GKdV equation is presented using phase plots. It is seen that the GKdV equation supports superperiodic traveling wave solution only and it is significantly affected by velocity and nonlinear parameters. Also, considering a superficial periodic forcing multistability of traveling waves of perturbed GKdV equation is presented. It is found that the perturbed GKdV equation supports coexisting chaotic and various quasiperiodic features with same parametric values at different initial conditions.

1. Introduction

Searching for analytic solutions of the nonlinear evolution equations (NLEEs) have long been the main theme of constant interest in mathematical and physical communities. These analytical solutions can skilfully narrate a variety of physical phenomena in various areas of applied sciences, such as plasma dynamics, fluid dynamics, applied mathematics and thus provide more information about the physical aspects of problems [1]. These nonlinear physical phenomena can be sensitively described by several nonlinear evolution equations (NEEs). In the last few decades, appreciable progress has been build in comprehension of the integrability and non-integrability of nonlinear evolution equations [2]. One of the important research areas of fluid mechanics is to study the dynamics of shallow water waves in the frame works of different NEEs, such as equal width (EW) equation, Burgers equation, generalized regularized long wave (RLW) equation, modified Burgers equation, generalized EW equation, generalized Korteweg-de Vries (KdV) equation and so on. Korteweg and de Vries [3] defined One of the most interesting NEEs (KdV equation) as

$$U_t + \varepsilon U U_x + \mu U_{xxx} = 0, \tag{1}$$

* Corresponding author.
E-mail addresses: sbgkarakoc@nevsehir.edu.tr (S.B.G. Karakoc), deryasucu@aksaray.edu.tr (D. Sucu).

https://doi.org/10.1016/j.cjph.2020.10.010
Received 16 April 2020; Received in revised form 1 September 2020; Accepted 25 October 2020
Available online 29 October 2020

which describe propagation of one dimensional shallow water wave. The KdV equation, which is one of the NEEs of third order with dispersion term, has a variety of tremendous applications to govern nonlinear waves in anharmonic crystals [4], waves inbubble liquid mixtures, dust-acoustic waves in plasmas, electron-acoustic waves in space and hot plasmas including nonlinear shallow water waves [5]. Fundamental characteristic of the KdV equation is that velocity of the solitary wave is comparable to its width and amplitude. Also, another particular feature of the KdV equation is that it can produce solitons and multi-soliton, which can keep their identities and properties after interaction and overtaking collisions [6]. The theory of solitons is a significant field in the areas of applied physics and applied mathematics. Some exact traveling solutions of the KdV equation were invented [7,8] and existence and uniqueness of these traveling solutions were examined introducing special initial function by Gardner et al. [9]. The KdV equation was solved analytically as a series solution by Adomian decomposition method [10]. Also, widely, appropriateness of these traveling solutions is restricted. For this reason, numerical wave solutions of the KdV equation are needful for several initial and boundary conditions to pattern lots of physical cases. Zabusky and Kruskal [11] were first to obtain it's numerical solutions using finite difference method. There exists various methods to solve the KdV equation utilizing numerical approaches, for instance finite difference method [12,13], finite element method [14–24], pseudospectral method [25], variational iteration method [26], the modified Bernstein polynomials [27], meshless method [28,29], heat balance integral method [30], consistent Riccati expansion (CRE) method [31], three different ansatze methods [32], complex forms for the Hirota's method [33], tanh expansion method [34] etc. were proposed for numerical treatment of the KdV equation.

Actually the KdV equation is a special status of the GKdV equation given by

$$U_t + \varepsilon U^p U_x + \mu U_{xxx} = 0, \tag{2}$$

which has need for the boundary conditions $\frac{\partial U}{\partial x} \rightarrow 0$as $|x| \rightarrow 0,$where $\varepsilon,$and $\mu$are physical parameters and the suffices $x$and $t$symbolize spatial and time differentiations, respectively. Numerical solution of the Eq. (2) is achieved with boundary conditions taken from

$$\begin{array}{ll} U(a,t) = 0, & U(b,t) = 0, \\ U_x(a,t) = 0, & U_x(b,t) = 0, \\ U_{xx}(a,t) = 0, & U_{xx}(b,t) = 0, \quad t > 0 \end{array} \tag{3}$$

and an initial condition

$$U(x,0) = f(x), \qquad a \leq x \leq b. \tag{4}$$

A class of fully discrete scheme for GKdV equation in a bounded domain $(0, L)$has studied by Sepúlveda and Villagrán [35]. A collocation algorithm and Adomian decomposition method are practiced to the equation by Ak et al. [36] and Ismail et al[37]., respectively.

The other specific case of the GKdV equation is the modified Korteweg-de Vries (MKdV) equation for $p = 2$. Recently a variety of numerical approaches have been upgraded for the traveling solution of the MKdV equation. The higher order GKdV equations with specific initial values were solved by implementing the Adomian decompositon method by Kaya [38]. Biswas et al[39].suggested Galerkins' solution for the MKdV equation utilizing quadratic B-splines. Numerical treatments of the MKDV equation have been introduced using Galerkin and Petrov Galerkin methods by Ak et al. [40,41]. Also Karakoc [42,43] has reported numerical traveling solutions for the MKdV equation utilizing subdomain and collocation methods. This study intends to prove that the presented numerical scheme is proficient of attaining significant precision for the problems symbolized by the generalized KdV equation.

A supernonlinear traveling wave is a nonlinear traveling wave distinguished by nontrivial topology of the phase spaces. Recently, supernonlinear traveling waves were reported in different physical systems, such as, waves in plasmas [44–47], optical pulses [48], etc. Investigating the dynamics of nonlinear evolution equation one can find out that few nonlinear systems can provide many solutions for a specific set of parameter values and distinct initial conditions [49–51]. This kind of nonlinear phenomenon is termed as multistability or existence of coexisting features. Multistability or coexisting features, as a new development area in the study of physical models, is on the path of its beginning. Therefore, the physical models with multistability behaviors need more studies. For the first time in the literature, we give these properties for the GKdV equation.

The aim of our study is to indicate that the suggested numerical scheme is proficient of succeeding high precision for the problem performed by the GKdV equation. Structure of this work contains Sections 1–7. Section 1 deals with the introductory section. Petrov-Galerkin method is explained and applied for getting the numerical solution of the GKdV equation in Section 2. Section 3 includes stability analysis of the method. Section 4 comprises probing of the motion of single solitary wave with several initial and boundary conditions. In Section 5, we study supernonlinear traveling wave solution of the GKdV equation using phase plane analysis. In Section 6, we present multistability of traveling wave solution of the perturbed GKdV equation utilizing external periodic forcing. Concluding remarks of this examination are proffered in Section 7.

2. Construction and application of the numerical method

The space domain $[a, b]$is portioned into $n$equal parts each of length $h$by the points $x_m,$ where $a = x_0 < x_1 < \ldots < x_N = b$.Prenter [52] defined cubic B-splines as follows

$$\phi_m(x)=\frac{1}{h^3}\begin{cases}(x-x_{m-2})^3, & x\in[x_{m-2},x_{m-1}),\\ h^3+3h^2(x-x_{m-1})+3h(x-x_{m-1})^2-3(x-x_{m-1})^3, & x\in[x_{m-1},x_m),\\ h^3+3h^2(x_{m+1}-x)+3h(x_{m+1}-x)^2-3(x_{m+1}-x)^3, & x\in[x_m,x_{m+1}),\\ (x_{m+2}-x)^3, & x\in[x_{m+1},x_{m+2}],\\ 0 & otherwise\end{cases} \tag{5}$$

and the set of cubic B-splines $\{\phi_{-1}(x),\ldots,\phi_{N+1}(x)\}$a basis over the region $[a,b]$. In the cubic B-spline Petrov-Galerkin method, we seek the approximation $U_N(x,t)$to the solution $U(x,t)$in the form

$$U_N(x,t)=\sum_{j=-1}^{N+1}\phi_j(x)\delta_j(t), \tag{6}$$

where $\delta_j(t)$are obtained using boundary and weighted residual conditions. When we appliying the transformation $h\eta=x-x_m$, $0\le\eta\le1$, cubic B-spline shape functions (5) having representations over the element $[x_m,x_{m+1}]$are obtained as

$$\begin{aligned}\phi_{m-1}&=(1-\eta)^3,\\ \phi_m&=1+3(1-\eta)+3(1-\eta)^2-3(1-\eta)^3,\\ \phi_{m+1}&=1+3\eta+3\eta^2-3\eta^3,\\ \phi_{m+2}&=\eta^3.\end{aligned} \tag{7}$$

Therefore approximation function (6) in terms of element parameters $\delta_{m-1},\delta_m,\delta_{m+1},\delta_{m+2}$and B-spline element functions $\phi_{m-1},\phi_m,\phi_{m+1},\phi_{m+2}$is given over the region [0,1] by

$$U_N(\eta,t)=\sum_{j=m-1}^{m+2}\delta_j\phi_j. \tag{8}$$

Also $U$and its space derivatives at the knots $x_m$can be obtained as

$$\begin{aligned}U_m&=U(x_m)=\delta_{m-1}+4\delta_m+\delta_{m+1},\\ U_m'&=U'(x_m)=3(-\delta_{m-1}+\delta_{m+1}),\\ U_m''&=U''(x_m)=6(\delta_{m-1}-2\delta_m+\delta_{m+1}).\end{aligned} \tag{9}$$

Now, we choose the weight function $\Phi_m$as the following quadratic B-splines [52]:

$$\Phi_m(x)=\frac{1}{h^2}\begin{cases}(x_{m+2}-x)^2-3(x_{m+1}-x)^2+3(x_m-x)^2, & x\in[x_{m-1},x_m),\\ (x_{m+2}-x)^2-3(x_{m+1}-x)^2, & x\in[x_m,x_{m+1}),\\ (x_{m+2}-x)^2, & x\in[x_{m+1},x_{m+2}),\\ 0 & otherwise.\end{cases} \tag{10}$$

When we use the transformation $h\eta=x-x_m$quadratic B-splines $\Phi_m$are found as

$$\begin{aligned}\Phi_{m-1}&=(1-\eta)^2,\\ \Phi_m&=1+2\eta-2\eta^2,\\ \Phi_{m+1}&=\eta^2.\end{aligned} \tag{11}$$

Practicing the Petrov-Galerkin method to Eq. (2), the weak form of Eq. (2) is procured as

$$\int_a^b\Phi(U_t+\varepsilon U^pU_x+\mu U_{xxx})dx=0. \tag{12}$$

When we use the transformation $h\eta=x-x_m(0\le\eta\le1)$for $[x_m,x_{m+1}]$in Eq. (12), we have the following integral equation:

$$\int_0^1\Phi\left(U_t+\varepsilon\left(\frac{U^p}{h}\right)U_\eta+\mu\left(\frac{1}{h^3}\right)U_{\eta\eta\eta}\right)d\eta=0. \tag{13}$$

If we take the integral of Eq. (13) using the Eq. (2) which yields:

$$\int_0^1[\Phi(U_t+\varepsilon\lambda U_\eta)-\beta\Phi_\eta U_{\eta\eta}]d\eta=-\beta\Phi U_{\eta\eta}|_0^1, \tag{14}$$

where $\lambda=\frac{U^p}{h}$and $\beta=\frac{\mu}{h^2}$.Substituting the expression (8) in Eq. (14) leads to

$$\sum_{j=m-1}^{m+2}[(\int_0^1\Phi_i\phi_jd\eta\ ]\dot{\delta}_j^e+\sum_{j=m-1}^{m+2}[(\varepsilon\lambda\int_0^1\Phi_i\phi_j'd\eta)-(\beta\int_0^1\Phi_i'\phi_j''d\eta)+(\beta\phi_i\phi_j''|_0^1)]\delta_j^e=0, \tag{15}$$

where $\delta^e = (\delta_{m-1}, \delta_m, \delta_{m+1}, \delta_{m+2})^T$ denote element parameters and dot shows differentiation to t which is written as follows:

$$[A^e]\dot{\delta}^e + [(\varepsilon\lambda B^e - \beta(C^e - D^e)]\delta^e = 0. \tag{16}$$

The element matrices $A^e_{ij}, B^e_{ij}, C^e_{ij}$ and D^e_{ij} are rectangular 3×4 given by the following integrals;

$$A^e_{ij} = \int_0^1 \Phi_i\phi_j d\eta = \frac{1}{60}\begin{bmatrix} 10 & 71 & 38 & 1 \\ 19 & 221 & 221 & 19 \\ 1 & 38 & 71 & 10 \end{bmatrix},$$

$$B^e_{ij} = \int_0^1 \Phi_i\phi_j' d\eta = \frac{1}{10}\begin{bmatrix} -6 & -7 & 12 & 1 \\ -13 & -41 & 41 & 13 \\ -1 & -12 & 7 & 6 \end{bmatrix},$$

$$C^e_{ij} = \int_0^1 \Phi_i'\phi_j'' d\eta = \begin{bmatrix} -4 & 6 & 0 & -2 \\ 2 & -6 & 6 & -2 \\ 2 & 0 & -6 & 4 \end{bmatrix},$$

$$D^e_{ij} = \Phi_i\phi_j''|_0^1 = \begin{bmatrix} -6 & 12 & -6 & 0 \\ -6 & 18 & -18 & 6 \\ 0 & 6 & -12 & 6 \end{bmatrix}.$$

We derive a lumped value of λ from $(\frac{U_m+U_{m+1}}{2}^p)$ as

$$\lambda = \frac{1}{4h}(\delta_{m-1} + 5\delta_m + 5\delta_{m+1} + \delta_{m+2})^p.$$

Assembling contributions from all elements generate the following system

$$[A]\dot{\delta} + [(\varepsilon\lambda B - \beta(C - D)]\delta = 0, \tag{17}$$

where $\delta = (\delta_{-1}, \delta_0, \ldots, \delta_N, \delta_{N+1})^T$ global element parameters. The $A, \lambda B, C$ and D matrices are rectangular and their each line of m are

$$A = \frac{1}{60}(1, 57, 302, 302, 57, 1, 0),$$
$$\lambda B = \frac{1}{10}\begin{pmatrix} -\lambda_1, -12\lambda_1 - 13\lambda_2, 7\lambda_1 - 41\lambda_2 - 6\lambda_3, 6\lambda_1 + 41\lambda_2 - 7\lambda_3, \\ 13\lambda_2 + 12\lambda_3, \lambda_3, 0 \end{pmatrix}$$
$$C = 2(1, 1, -8, 8, -1, -1, 0), \quad D = (0, 0, 0, 0, 0, 0, 0)$$

where

$$\lambda_1 = \frac{1}{4h}(\delta_{m-2} + 5\delta_{m-1} + 5\delta_m + \delta_{m+1})^p, \ \lambda_2 = \frac{1}{4h}(\delta_{m-1} + 5\delta_m + 5\delta_{m+1} + \delta_{m+2})^p,$$
$$\lambda_3 = \frac{1}{4h}(\delta_m + 5\delta_{m+1} + 5\delta_{m+2} + \delta_{m+3})^p.$$

Using the Crank–Nicholson formulation $\delta_m = \frac{1}{2}(\delta^n + \delta^{n+1})$ and usual finite difference approximation $\dot{\delta}_m = \frac{\delta^{n+1}-\delta^n}{\Delta t}$ into Eq. (17) leads to the following iterative relationship

$$\left[A + \varepsilon\lambda B - \beta(C - D)\frac{\Delta t}{2}\right]\delta^{n+1} = \left[A - \varepsilon\lambda B - \beta(C - D)\frac{\Delta t}{2}\right]\delta^n. \tag{18}$$

Practicing the boundary conditions (3) to the Eq. (18), $(N+1)\times(N+1)$ matrix system is obtained and can be solved using the Thomas algorithm. Consequently, a representative member of the (18) is written as

$$\begin{aligned} &\rho_1\delta^{n+1}_{m-2} + \rho_2\delta^{n+1}_{m-1} + \rho_3\delta^{n+1}_m + \rho_4\delta^{n+1}_{m+1} + \rho_5\delta^{n+1}_{m+2} + \rho_6\delta^{n+1}_{m+3} = \\ &\rho_6\delta^n_{m-2} + \rho_5\delta^n_{m-1} + \rho_4\delta^n_m + \rho_3\delta^n_{m+1} + \rho_2\delta^n_{m+2} + \rho_1\delta^n_{m+3}, \end{aligned} \tag{19}$$

where

$$\rho_1 = \frac{1}{60} - \frac{\varepsilon\lambda\Delta t}{20} - \beta\Delta t, \qquad \rho_2 = \frac{57}{60} - \frac{25\varepsilon\lambda\Delta t}{20} - \beta\Delta t,$$
$$\rho_3 = \frac{302}{60} - \frac{40\varepsilon\lambda\Delta t}{20} + 8\beta\Delta t, \quad \rho_4 = \frac{302}{60} + \frac{40\varepsilon\lambda\Delta t}{20} - 8\beta\Delta t,$$
$$\rho_5 = \frac{57}{60} + \frac{25\varepsilon\lambda\Delta t}{20} + \beta\Delta t, \quad \rho_6 = \frac{1}{60} + \frac{\varepsilon\lambda\Delta t}{20} + \beta\Delta t.$$

To begin the solution procedure, we require to obtain initial parameters δ_m^0.Considering Eqs. (3) and (4), values of initial parameters δ_m^0at the initial time are found with the following relations

$$\begin{aligned} U_N(x_m,0) &= U(x_m,0), \\ U_N^{'}(x_0,0) &= U^{'}(x_N,0)=0. \end{aligned}$$

So the initial parameters δ_m^0can be calculated from the following equation

$$\begin{bmatrix} -3 & 0 & 3 & & & \\ 1 & 4 & 1 & & & \\ & & \ddots & & & \\ & & & 1 & 4 & 1 \\ & & & -3 & 0 & 3 \end{bmatrix} \begin{bmatrix} \delta_{-1}^0 \\ \delta_0^0 \\ \vdots \\ \delta_N^0 \\ \delta_{N+1}^0 \end{bmatrix} = \begin{bmatrix} U^{'}(x_0,0) \\ U(x_0,0) \\ \vdots \\ U(x_N,0) \\ U^{'}(x_N,0) \end{bmatrix}.$$

3. Stability analysis

Von Neumann stability analysis will be performed and growth of a Fourier mode $\delta_j^n = \kappa^n e^{ijkh}, (i = \sqrt{-1})$where $k$denotes mode number and $h$denotes element size, which can be obtained using linearisation of numerical approach. Utilizing the Fourier mode in Eq. (19) with some arrangements, the growth factor is generated as

$$\kappa = \frac{X - iY}{X + iY}, \tag{20}$$

where

$$\begin{aligned} X &= 302\cos\left(\frac{\theta}{2}\right) + 57\cos\left(\frac{3\theta}{2}\right) + \cos\left(\frac{5\theta}{2}\right), \\ Y &= [(120\varepsilon\lambda - 480\beta)\Delta t]\sin\left(\frac{\theta}{2}\right) + [(75\varepsilon\lambda + 60\beta)\Delta t]\sin\left(\frac{3\theta}{2}\right) + \\ &\quad [(3\varepsilon\lambda + 60\beta)\Delta t]\sin\left(\frac{5\theta}{2}\right). \end{aligned} \tag{21}$$

and $\theta = kh$.Since $|\kappa|$is 1, our method is neutrally stable.

4. Numerical applications

Now we present a number of problems to validate the applicability of the method. For this reason, we obtain numerical solution of Eq. (2) for $p = 1, 2$and 3.

$$L_2 = \| U^{exact} - U_N \|_2 \simeq \sqrt{h \sum_{J=0}^{N} \left| U_j^{exact} - (U_N)_j \right|^2},$$

and

$$L_\infty = \| U^{exact} - U_N \|_\infty \simeq \max_j \left| U_j^{exact} - (U_N)_j \right|,$$

error norms are used to measure the accuracy of the present algorithm and to compare our result with existing literature. Analytic solution of the GKdV equation is found [36,37] to be

$$U(x,t) = A\mathrm{sech}^2[k(x - x_0 - ct)]^{\frac{1}{p}},$$

where $A = \left[\frac{c(p+1)(p+2)}{2\varepsilon}\right]$and $k = \frac{p}{2}\sqrt{\frac{c}{\mu}}$.

The GKdV equation provides many invariant polynomials which can be procured systematically as follows

$$I_1 = \int_a^b U(x,t)dx, \quad I_2 = \int_a^b \left[U^2(x,t)\right]dx, \quad I_3 = \int_a^b \left[U^{p+2}(x,t) - \frac{\mu(p+1)(p+2)}{2\varepsilon}(U_x(x,t))^2\right]dx. \tag{22}$$

After computing solitary wave profile, we can observe values of I_1,$I_2$and I_3which can be used to verify the accuracy of the proposed computational numerical approach.

4.1. Propagation of a single solitary wave

In this part, different numerical examples will be given to illustrate the efficiency and accuracy of the method. For the GKdV equation, parameters used by earlier authors to obtain their results are taken as guiding principle for our calculations.

4.2. Case 1

For the first case, behavior of the solutions are investigated with two sets of parameters, $p=1,\varepsilon=1,\mu=4.84\times10^{-4},c=0.3,h=0.01,\Delta t=0.005,x\in[0,2]$and $\varepsilon=3,\mu=1,c=0.3,h=0.1,\Delta t=0.01,x\in[0,80]$to coincide with the previous works [4,14–19,29,36]. So, solitary waves have amplitude 0.9 and 0.3, respectively and our scheme is executed up to $t=1$.We calculate values of the error norms and invariants for different time levels and compare them with earlier papers in Table 1. It is seen that our algorithm provides good results than most of the others. We have got change of the values of the invariants $0,0,2.8\times10^{-5}$for $\mu=4.84\times10^{-4}$; 2×10^{-6}, 0, 0 for $\mu=1$and the error norms remain less than $0.920633\times10^{-3}$and $2.783765\times10^{-3}$for $\mu=4.84\times10^{-4}$and 0.018×10^{-3},$0.017\times10^{-3}$for $\mu=1$. Numerical solutions are exhibited at different time levels in Fig. 1. Distribution of errors at time $t=1$are depicted in Fig. 2. The error deviations for different valus of μvaries from $-3\times10^{-3}$to $4\times10^{-3}$and $-2\times10^{-5}$to 5×10^{-6}, respectively.

4.3. Case 2

We introduce the numerical results for the second case $p=2,\varepsilon=3,\mu=1,h=0.1,\Delta t=0.01,c=0.845$and $c=0.3,h=0.1,\Delta t=0.01,x\in[0,80]$.Then solitary waves have amplitudes 1.3416 and 0.7746, respectively and our scheme is executed up to $t=20$and $t=1$.The three invariants and the errors norms are summarized in Table 2. We have got change of the values of the invariants 0, 0 and $2.61\times10^{-3}$for $c=0.845$; 2×10^{-6},0,$4\times10^{-5}$for $c=0.3$and the error norms remain less than 1.969104×10^{-3},$1.301272\times10^{-3}$for $c=0.845$and 0.105×10^{-3},$0.052\times10^{-3}$for $c=0.3$respectively, throughout the simulation. Fig. 3 shows the solution profiles for $t=0,5,10,15,20$and $t=0,0.1,0.2\ldots,1$, respectively. To indicate the errors between the exact and numerical results over the solution interval, error distributions at time $t=20$and $t=1$is depicted graphically in Fig. 4.

4.4. Case 3

We present the numerical results for the final case $p=3,\varepsilon=3,\mu=1,h=0.01,\Delta t=0.005,c=0.845$and $c=0.3,h=0.1,\Delta t=0.01,x\in[0,80]$.These specific values provide the amplitudes 1.4122 and 1.0000, respectively and our scheme is executed up to $t=20$and $t=1$.All results are documented in Table 3. Referring to Table 3, we have got change of the values of the invariants 0, 0 and $1.17\times10^{-2}$for $c=0.845$; 3×10^{-6}, 0, $3.3\times10^{-4}$for $c=0.3$and the error norms remain less than 9.989772×10^{-3}, $6.843777\times10^{-3}$for $c=0.845$and 0.238×10^{-3}, $0.129\times10^{-3}$for $c=0.3$respectively, throughout the simulation. For visual representation,

Table 1
Comparisons of results for invariants and error norms with $p=1,\varepsilon=1,\mu=4.84\times10^{-4},c=0.3,h=0.01,\Delta t=0.005,x\in[0,2]$and $\varepsilon=3,\mu=1,c=0.3,h=0.1,t=0.01,x\in[0,80]$,.

Method	Time	I_1	I_2	I_3	$L_2\times10^3$	$L_\infty\times10^3$
$\mu=4.84\times10^{-4}$Present Method	0.00	0.144598	0.086759	0.046850	0	0
	0.25	0.144598	0.086759	0.046755	0.404868	0.906618
	0.50	0.144598	0.086759	0.046625	0.545796	1.537960
	0.75	0.144598	0.086759	0.046914	0.719048	2.160523
	1.00	0.144598	0.086759	0.046878	0.920633	2.783765
[4]					28.66	
[14] Septic Coll.	1.00	0.14460	0.086759	0.046877	22.1	
[15]	1.00	0.144592	0.086759	0.016870	22.2	
[16] P-G	1.00				0.75	
[16] Modified P-G	1.00				4.33	
[17]	1.00				18.72	
[18]	1.00				29.45	
[19]	1.00				63.72	
[29] MQ	1.00	0.144606	0.086759	0.046850	0.062	0.133
[29] IMQ	1.00	0.144623	0.086765	0.046847	2.751	5.018
[29] IQ	1.00	0.144598	0.086759	0.046849	1.013	2.090
[29]TPS	1.00	0.144261	0.086762	0.046842	2.606	6.345
[29] G	1.00	0.144601	0.086760	0.046850	0.046	0.136
[36]	1.00	0.144599	0.086759	0.046850	0.079	0.238
$\mu=1$Present Method	0.00	2.190842	0.438176	0.078871	0	0
	0.25	2.190844	0.438176	0.078871	0.013	0.020
	0.50	2.190844	0.438176	0.078871	0.015	0.019
	0.75	2.190844	0.438176	0.078871	0.016	0.018
	1.00	2.190844	0.438176	0.078871	0.018	0.017

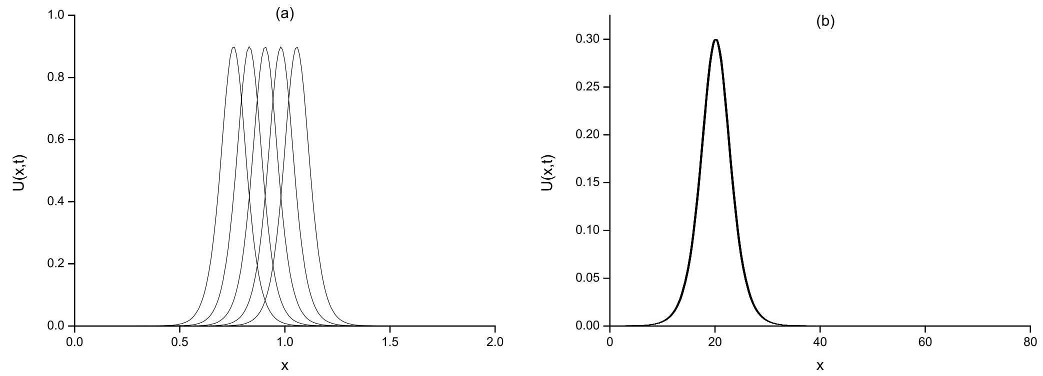

Fig. 1. Movement of single solitary wave (MOSSW) profile for a) $p = 1, \varepsilon = 1, \mu = 4.84 \times 10^{-4}, c = 0.3, h = 0.01, \Delta t = 0.005$and b) $\varepsilon = 3, \mu = 1, c = 0.3, h = 0.1, \Delta t = 0.01$.

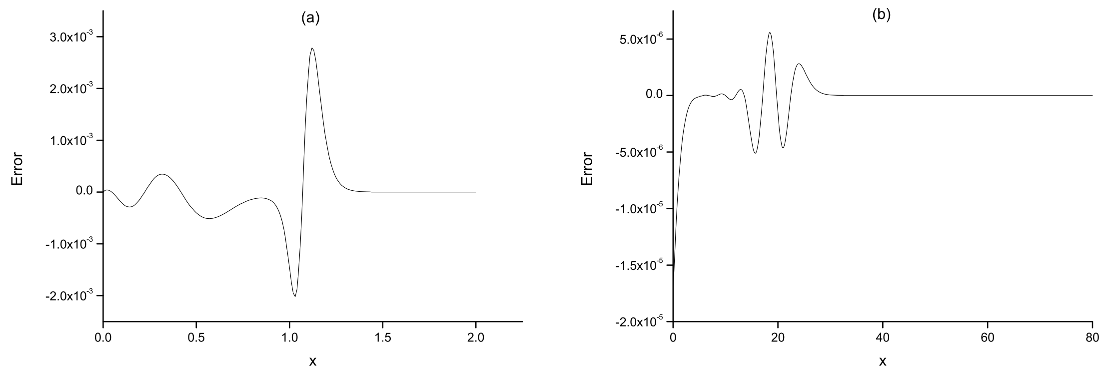

Fig. 2. Error distributions at $t = 1$for the parameters a) $p = 1, \varepsilon = 1, \mu = 4.84 \times 10^{-4}, c = 0.3, h = 0.01, \Delta t = 0.005$and b) $\varepsilon = 3, \mu = 1, c = 0.3, h = 0.1, \Delta t = 0.01$.

Table 2
Comparisons of results for invariants and error norms with $p = 2, \varepsilon = 3, \mu = 1, h = 0.1, \Delta t = 0.01, c = 0.845$and $c = 0.3, h = 0.1, \Delta t = 0.01$.

Method	*Time*	I_1	I_2	I_3	$L_2 \times 10^3$	$L_\infty \times 10^3$
$c = 0.845$Present Method	0	4.442865	3.676941	2.071335	0	0
	5	4.442865	3.676941	2.073762	0.916736	0.561271
	10	4.442865	3.676941	2.073904	1.260179	0.846318
	15	4.442865	3.676941	2.073934	1.628483	1.090379
	20	4.442865	3.676941	2.073953	1.969104	1.301272
[39]	20	4.443171	3.679192	2.077161	-	8.642137
[40]	20	4.442866	3.676941	2.073841	3.656694	2.294197
[41]	20	4.442866	3.676941	2.073846	3.641638	2.285638
[42]	1	4.442863	3.676933	2.071312	830.4	480.5
[43]	1	4.442865	3.676941	2.071327	0.0184	0.0117
$c = 0.3$Present Method	0.00	4.442815	2.190881	0.438173	0	0
	0.25	4.442817	2.190881	0.438179	0.047	0.030
	0.50	4.442817	2.190881	0.438191	0.073	0.043
	0.75	4.442817	2.190881	0.438202	0.092	0.049
	1.00	4.442817	2.190881	0.438213	0.105	0.052
[42]	1.00	4.442765	2.190882	0.438173	140.1	635.5
[43]	1.00	4.44285	2.1908	0.438146	0.107	0.200

behaviors of solutions at times $t = 0, 5, 10, 15, 20$and $t = 0, 0.1, \ldots, 1$are depicted in Fig. 5. Distributions of specific errors at time $t = 20$and $t = 1$are graphed in Fig. 6.

5. Supernonlinear wave

We investigate supernonlinear traveling wave solution of Eq. (2) for the first time in literature. To explore all possible

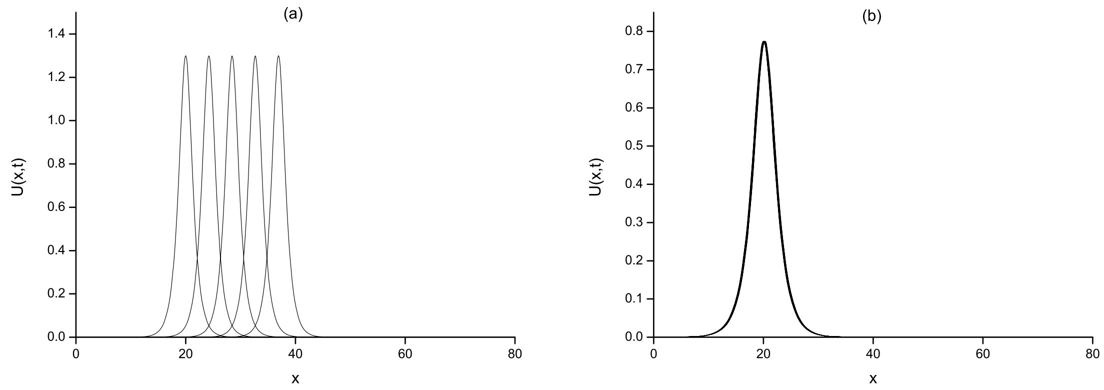

Fig. 3. MOSSW for a) $p = 2, \varepsilon = 3, \mu = 1, h = 0.1, \Delta t = 0.01, c = 0.845$and b) $c = 0.3, h = 0.1, \Delta t = 0.01$.

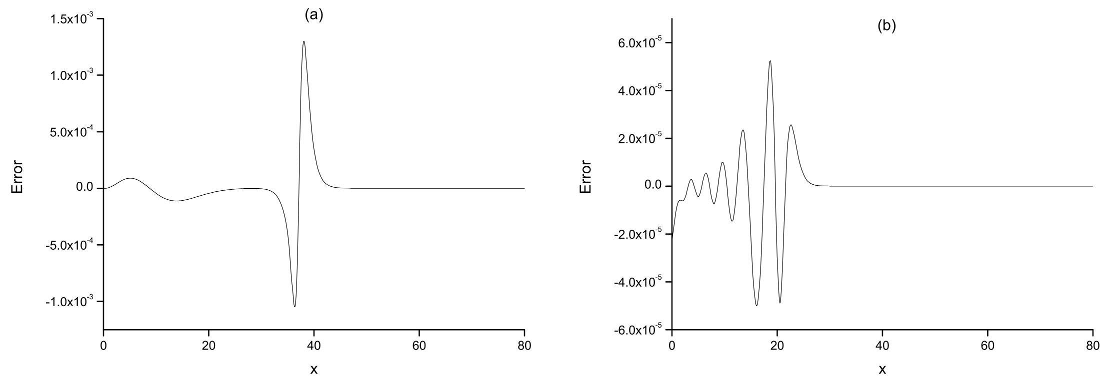

Fig. 4. Error distributions for the parameters a) $p = 2, \varepsilon = 3, \mu = 1, h = 0.1, \Delta t = 0.01, c = 0.845, t = 20$and b) $c = 0.3, h = 0.1, \Delta t = 0.01, t = 1$.

Table 3
Values of the invariants and error norms for $p = 3, \varepsilon = 3, \mu = 1, h = 0.01, \Delta t = 0.005, c = 0.845$and $c = 0.3, h = 0.1, \Delta t = 0.01$.

Method	*Time*	I_1	I_2	I_3	$L_2 \times 10^3$	$L_\infty \times 10^3$
$c = 0.845$Present Method	0	4.308401	3.742115	1.505761	0	0
	5	4.308401	3.742115	1.515932	1.928209	1.346190
	10	4.308401	3.742115	1.517105	4.307469	2.973856
	15	4.308401	3.742115	1.517411	7.225562	4.847671
	20	4.308401	3.742115	1.517513	9.989772	6.843777
$c = 0.3$Present Method	0.00	5.119973	3.148917	0.449836	0	0
	0.25	5.119976	3.148917	0.449938	0.132	0.091
	0.50	5.119976	3.148917	0.450038	0.185	0.112
	0.75	5.119976	3.148917	0.450111	0.216	0.119
	1.00	5.119976	3.148917	0.450171	0.238	0.129

supernonlinear traveling waves of Eq. (2), one can employ a frame $\xi = x - vt$with speed v. Then Eq. (2)becomes

$$-vU_\xi + \varepsilon U^p U_\xi + \mu U_{\xi\xi\xi} = 0. \tag{23}$$

Performing integration inequation (23), we derive

$$-vU + \frac{\varepsilon}{p+1} U^{p+1} + \mu U_{\xi\xi} = c, \tag{24}$$

here c denotes an integrating constant. Applying the boundary conditions $U \to 0,\ U_\xi \to 0, U_{\xi\xi} \to 0$as $\xi \to \pm\infty$, we have

$$-vU + \frac{\varepsilon}{p+1} U^{p+1} + \mu U_{\xi\xi} = 0. \tag{25}$$

Then the system (25) is written as the following dynamical system (DS):

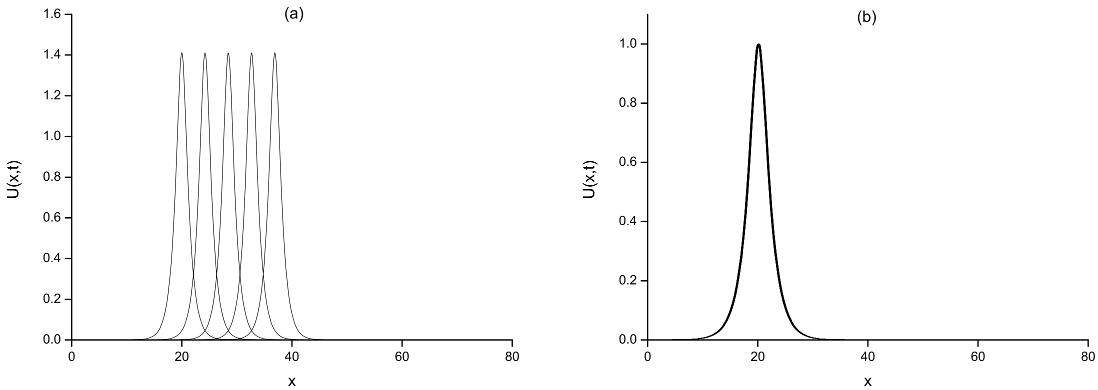

Fig. 5. MOSSW for a) $p = 3, \varepsilon = 3, \mu = 1, h = 0.01, \Delta t = 0.005, c = 0.845$and b) $c = 0.3, h = 0.1, \Delta t = 0.01$.

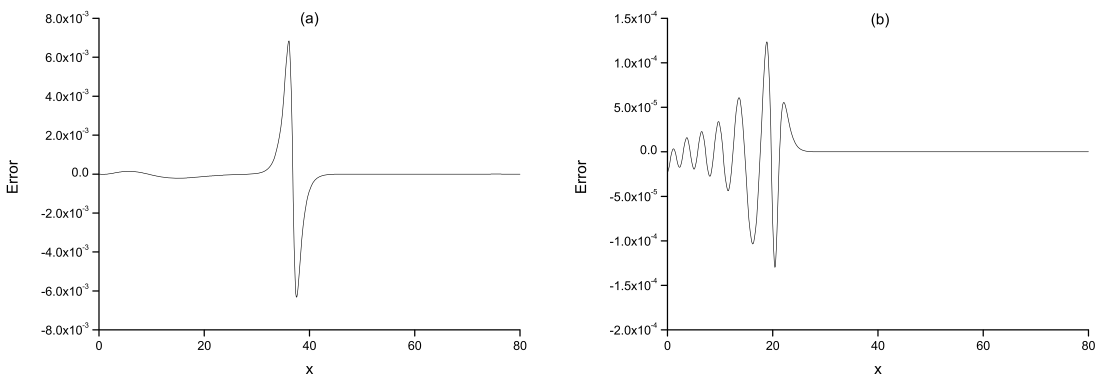

Fig. 6. Error distributions for the parameters a) $p = 3, \varepsilon = 3, \mu = 1, h = 0.01, \Delta t = 0.005, c = 0.845, t = 20$and b) $c = 0.3, h = 0.1, \Delta t = 0.01, t = 1$.

$$\begin{aligned} U_\xi &= Z, \\ Z_\xi &= U(A - BU^p), \end{aligned} \tag{26}$$

where $A = \frac{v}{\mu}$and $B = \frac{\varepsilon}{\mu(p+1)}$. The system (26)is a planar Hamiltonian system [53–57] with $\omega_0$and $v$as physical parameters. If $p$is an odd integer, then the DS (26) has two singular points at $E_0(U_0, 0)$and $E_1(U_1, 0)$, where $U_0 = 0$and $U_1 = \left(\frac{A}{B}\right)^{1/p}$. If $p$is an even integer, then the DS (26) has three singular points at $E_0(U_0, 0), E_1(U_1, 0)$and $E_2(U_2, 0)$, where $U_0 = 0, U_1 = \left(\frac{A}{B}\right)^{1/p}$ and $U_2 = -\left(\frac{A}{B}\right)^{1/p}$.

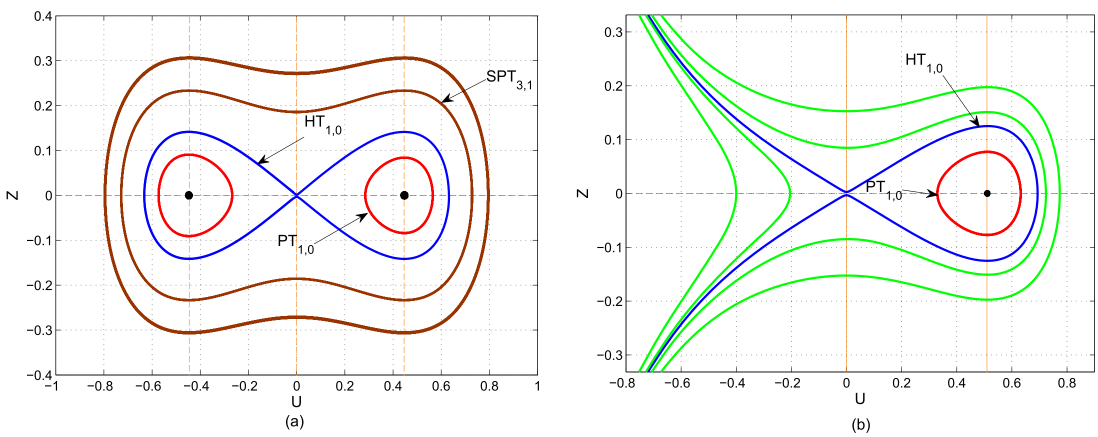

Fig. 7. Phase plot of the DS (26) for: (a) $p = 2, \varepsilon = 3, \mu = 1, v = 0.2$and (b) $p = 3, \varepsilon = 3, \mu = 1, v = 0.1$.

The Hamiltonian function corresponding to the DS (26) is defined as

$$H(U,Z)=\frac{Z^2}{2}-\frac{A}{2}U^2+\frac{B}{p+1}U^{(p+1)}=h. \tag{27}$$

For each point (U_i,Z_i) in the UZ-plane, the equation $H(U,Z)=h$represents a trajectory which corresponds to a traveling wave of Eq. (2).

In Fig. 7 (a), phase plot of the DS (26) is presented for $p=2,\varepsilon=3,\mu=1,$and $v=0.2$. It contains three kinds of distinct trajectories which are qualitatively different, namely, two opposite homoclinic trajectories ($HT_{1,0}$) at the singular point $E_0(0,0)$,two collections of periodic trajectories ($PT_{1,0}$) surrounding the centers at the singular points $E_1(U_1,0)$and $E_2(U_2,0)$and a family of superperodic trajectories ($SPT_{3,1}$). In Fig. 7(b), phase plot of the DS (26) is presented for $p=3,\varepsilon=3,\mu=1,$and $v=0.1$. This phase plot contains two types of distinct trajectories which are qualitative different, namely, a homoclinic trajectory ($HT_{1,0}$) at the singular point $E_0(0,0)$and one family of periodic trajectories ($PT_{1,0}$) surrounding the center at $E_1(U_1,0)$.

In Fig. 8 (a), effect of velocity (v) of traveling wave is shown on supernonlinear traveling wave of the GKdV Eq. (2). It is perceived that as $v$is enhanced, amplitude of supernonlinear traveling wave grows and its width reduces. As a result the supernonlinear traveling wave of the GKdV Eq. (2) becomes spiky. In Fig. 8 (b), effect of nonlinear parameter (ε) of traveling wave is shown on supernonlinear traveling wave of the GKdV Eq. (2). It is seen that as εincreases, amplitude and width of supernonlinear traveling wave decrease. As a result the supernonlinear traveling wave of the GKdV Eq. (2) diminishes.

6. Multistability

Recently, effect of external source term on traveling waves is reported [58]. Such nonlinear source term as a superficial forcing, is of various types [59,60]. We consider a superficial forcing term as $f_0\cos(\omega\xi)$. So, introducing superficial forcing $f_0\cos(\omega\xi)$ to the system (26), one can acquire the perturbed dynamical system (PDS) as

$$\begin{aligned} U_\xi &= Z,\\ Z_\xi &= U(A-BU^p)+f_0\,cos(\omega\xi), \end{aligned} \tag{28}$$

here $f_0(\omega)$ denote strength (frequency) of the superficial forcing.

In Fig. 9 (a), coexisting orbits of the PDS (28) are presented for same parametric values $p=2,\varepsilon=3,\mu=1,$and $v=0.2$with various initial conditions. Chaotic orbit is presented by blue curve at an initial condition $(U,Z)=(0,0.2)$. Three different types of quasiperiodic orbits are presented at three different initial conditions with curves of various colours: $(U,Z)=(0,0.8)$(red curve), $(U,Z)=(0,1.2)$(green curve), and $(U,Z)=(0,1.8)$(magenta curve). In Fig. 9 (b), corresponding time series plots of the PDS (28) are presented for same situations as Fig. 9 (a). This confirms the existence of multistability behavior of nonlinear waves of the GKdV Eq. (2) in appearance of superficial forcing.

7. Conclusion

In this work, Petrov-Galerkin method are presented to numerically solve the GKdV equation. The obtained numerical results proved that our error norms reasonably small or too close to the results in literature and the conservation properties remain almost constant

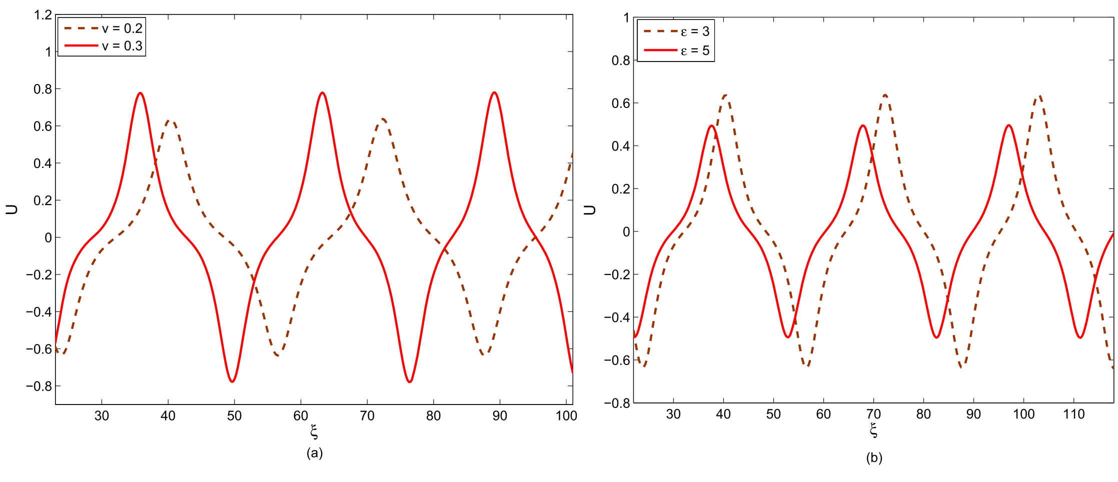

Fig. 8. Superperiodic wave solution of Eq. (2) for: (a) $p=2,\varepsilon=3,\mu=1,v=0.2$(brown curve), $v=0.3$(red curve), and (b) $p=2,\mu=1,v=0.2,\epsilon=3$(brown curve), $\epsilon=5$(red curve). (For interpretation of the references to color in this figure legend, the reader is referred to the web version of this article.)

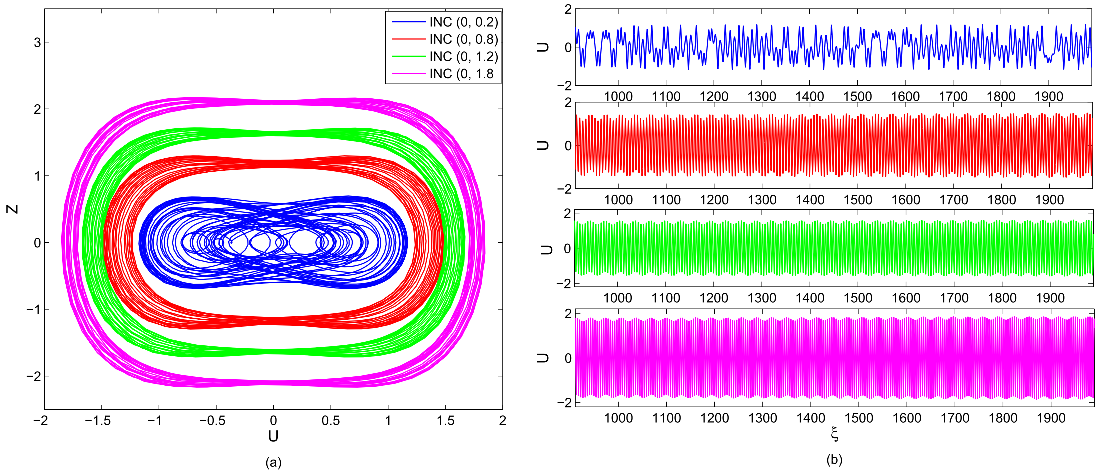

Fig. 9. Multistability of the system (28): (a) phase plot for $p = 2, \varepsilon = 3, \mu = 1, \nu = 0.2$with various initial conditions (INCs) and (b) time series plots for same parameters and INCs as Fig. 9 (a).

during the computer run. Moreover, the views of the solitary wave are alike to those of references. Numerical algorithms indicated that our scheme is unconditionally stable. Supernonlinear traveling wave solution of the GKdV equation has been perceived employing variation of $U$and phase plots. It has been found that the GKdV equation supports superperiodic traveling wave solution. The obtained superperiodic traveling wave solution has been affected significantly by velocity and nonlinear parameters. Furthermore, considering external periodic forcing multistability of traveling wave solution of the perturbed GKdV equation has been presented. It has been discovered that the GKdV equation with superficial forcing supports coexisting chaotic and various quasiperiodic features with same parametric values at different initial conditions.

Declaration of Competing Interest

The authors declare that they have no known competing financial interests or personal relationships that could have appeared to influence the work reported in this paper.

References

[1] M.A. Abdou, The extended f-expansion method and its application for a class of nonlinear evolution equations, Chaos, Solitons & Fractals 31 (2007) 95–104, https://doi.org/10.1016/j.chaos.2005.09.030.
[2] J. Sarma, Exact solutions for modified korteweg–de vries equation, Chaos, Solitons and Fractals 42 (2009) 1599–1603, https://doi.org/10.1016/j.chaos.2009.03.041.
[3] D.J. Korteweg, G. de Vries, On the change of form of long waves advancing in a rectangular canal and on a new type of long stationary waves, Philos. Mag. 39 (1895) 422–443, https://doi.org/10.1080/14786449508620739.
[4] N.J. Zabusky, A synergetic approach to problem of nonlinear dispersive wave propagation and interaction. Proceedings of the Symposium Nonlinear Partial Differential Equation, Academic Press, 1967, pp. 223–258, https://doi.org/10.1016/B978-1-4831-9647-3.50019-4.
[5] M. Sarboland, A. Aminataei, On the numerical solution of the nonlinear korteweg–de vries equation, Syst. Sci. Control Eng. 3 (2015) 69–80, https://doi.org/10.1080/21642583.2014.986340.
[6] A. Korkmaz, Numerical algorithms for solutions of korteweg–de vries equation, Numer. Method. Partial Differ. Equ. 26 (2010) 1504–1521, https://doi.org/10.1002/num.20505.
[7] B. Saka, Cosine expansion-based differential quadrature method for numerical solution of the KdV equation, Chaos, Solitons and Fractals 40 (2009) 2181–2190, https://doi.org/10.1016/j.chaos.2007.10.004.
[8] R.K. Dodd, J.C. Eilbeck, J.D. Gibbon, H.C. Morris, Solitons and Nonlinear Wave Equations, Academic Press, New York, 1982.
[9] C.S. Gardner, J.M. Green, M.D. Kruskal, R.M. Miura, Method for solving Korteweg–de Vries equation, Phys. Rev. Lett. 19 (1967) 1095–1097, https://doi.org/10.1103/PhysRevLett.19.1095.
[10] A.M. Wazwaz, Construction of solitary wave solutions and rational solutions for the KdV equation by Adomian decomposition method, Chaos, Solitons and Fractals 12 (2001) 2283–2293, https://doi.org/10.1016/S0960-0779(00)00188-0.
[11] N.J. Zabusky, M.D. Kruskal, Interaction of solitons in a collisionless plasma and the recurrence of initial states, Phys. Rev. Lett. 15 (1965) 240–243, https://doi.org/10.1103/PhysRevLett.15.240.
[12] K. Goda, On instability of some finite difference schemes for Korteweg-de Vries equation, J.Phys. Soc. Japan. 39 (1975) 229–236, https://doi.org/10.1143/JPSJ.39.229.
[13] A.C. Vliengenthart, On finite difference methods for the Korteweg-de Vries equation, J. Eng. Math. 5 (1971) 137–155, https://doi.org/10.1007/BF01535405.
[14] A.A. Soliman, Collocation solution of the Korteweg-de Vries equation using septic splines, Int. J. Comput. Math. 81 (2004) 325–331, https://doi.org/10.1080/00207160410001660817.
[15] A.A. Soliman, A.H.A. Ali, K.R. Raslan, Numerical solution for the KdV equation based on similarity reductions, Appl Math Model 33 (2009) 1107–1115, https://doi.org/10.1016/j.apm.2008.01.004.
[16] J.M.S. Serna, I. Christie, Petrov galerkin methods for non linear dispersive wave, J. Comput. Phys. 39 (1981) 94–102, https://doi.org/10.1016/0021-9991(81)90138-8.
[17] I.S. Greig, J.L. Morris, A hopscotch method for the Korteweg-de-Vries equation, J. Computational Phys. 20 (1976) 64–80, https://doi.org/10.1016/0021-9991(76)90102-9.
[18] L.R.T. Gardner, G.A. Gardner, A.H.A. Ali, A finite element solution for the Korteweg–de Vries equation with cubic b-splines, UCNW Math. Preprint 89.01 (1989).

[19] G.A. Gardner, L.R.T. Gardner, A.H.A. Ali, Modelling solutions of the Korteweg–de Vriesequation with quintic splines, UCNW Math. Preprint 90.30 (1990).
[20] I. D. Irk, I. Dağ, B. Saka, A small time solutions for the Korteweg–de Vriesequation using spline approximation, Appl. Math. Comput. 173 (2006) 834–846, https://doi.org/10.1016/j.amc.2005.04.018.
[21] A. Canıvar, M. Sarı, I. Dağ, A taylor-galerkin finite element method for the kdv equation using cubic b-splines, Phys. B 405 (2010) 3376–3383, https://doi.org/10.1016/j.physb.2010.05.008.
[22] O. Ersoy, I. Dağ, The exponential cubic B-spline algorithm for Korteweg-de Vries equation, Adv. Numer. Anal. 2015 (2015) 1–8, https://doi.org/10.1155/2015/367056.
[23] E.N. Aksan, A. Ozdes, Numerical solution of Korteweg–de Vries equation by Galerkin B-spline finite element method, Appl. Math. Comput. 175 (2006) 1256–1265, https://doi.org/10.1016/j.amc.2005.08.038.
[24] D. Irk, Quintic b-spline Galerkin method for the KdVequation, Anadolu Univ. J. Sci. Technol. B- Theorit. Sci. 5 (2017) 111–119, https://doi.org/10.20290/aubtdb.289203.
[25] B. Fornberg, G.B. Whitham, A numerical and theoretical study of certain nonlinear wave phenomena, Philos. Trans. Roy. Soc. 289 (1978) 373–404, https://doi.org/10.1098/rsta.1978.0064.
[26] M. Inc, Numerical simulation of KdV and mKdV equations with initial conditions by the variational iteration method, Chaos Soliton Fractals 34 (2007) 1075–1081, https://doi.org/10.1016/j.chaos.2006.04.069.
[27] D.D. Bhatta, M.I. Bhatti, Numerical solution of KdV equation using modified Bernstein polynomials, Appl. Math. Comput. 174 (2006) 1255–1268, https://doi.org/10.1016/j.amc.2005.05.049.
[28] C. Franke, R. Schaback, Solving partial differential equations by collocation using radial basis functions, Appl. Math. Comput. 93 (1998) 73–82, https://doi.org/10.1016/S0096-3003(97)10104-7.
[29] I. Dağ, Y. Dereli, Numerical solutions of KdV equation using radial basis function, Appl. Math. Model. 32 (2008) 535–546, https://doi.org/10.1016/j.apm.2007.02.001.
[30] S. Kutluay, A.R. Bahadır, A. Ozdes, A small time solutions for the Korteweg–de Vriesequation, Appl. Math. Comput 107 (2000) 203–210, https://doi.org/10.1016/S0096-3003(98)10119-4.
[31] W. Cheng, T. Xu, Consistent Riccati expansion solvable classification and solitoncnoidal wave interaction solutions for an extended Korteweg-de Vries equation, Chin. J. Phys. 56 (2018) 2753–2759, https://doi.org/10.1016/j.cjph.2018.09.032.
[32] M. Alquran, I. Jaradat, D. Baleanu, Shapes and dynamics of dual-mode Hirota–Satsuma coupled KdV equations: exact traveling wave solutions and analysis, Chin. J. Phys. 58 (2019) 49–56, https://doi.org/10.1016/j.cjph.2019.01.005.
[33] A.M. Wazwaz, Multiple complex soliton solutions for the integrable KdV, fifthorder Lax, modified KdV, burgers, and Sharma–Tasso–Olver equations, Chin. J. Phys. 59 (2019) 372–378, https://doi.org/10.1016/j.cjph.2019.03.001.
[34] Y.H. Wang, H. Wang, A coupled KdV system: consistent tanh expansion, soliton-cnoidal wave solutions and nonlocal symmetries, Chin. J. Phys. 56 (2018) 598–604, https://doi.org/10.1016/j.cjph.2018.02.009.
[35] M. Sepúlveda, O.V. Villagrán, Numerical Methods for Generalized Kdv Equations. In Anais do XXXI Congresso Nacional de Matematica Aplicada e Computacional, 2008, pp. 894–900.
[36] T. Ak, H. Triki, S. Dhawan, S.K. Bhowmik, S.P. Moshokoae, M.Z. Ullah, A. Biswas, Computational analysis of shallow water waves with Korteweg-de Vries equation, Scientia Iranica B 25 (2017) 2582–2597, https://doi.org/10.24200/SCI.2017.4518.
[37] H.N.A. Ismail, K.R. Raslan, G.S.E. Salem, Solitary wave solutions for the general KdVequation by Adomian decomposition method, Appl. Math. Comput. 154 (2004) 17–29, https://doi.org/10.1016/S0096-3003(03)00686-6.
[38] D. Kaya, An application for the higher order modified KdVequation by decomposition method, Commun. Nonlinear Sci. Num. Simul. 10 (2005) 693–702, https://doi.org/10.1016/j.cnsns.2003.12.009.
[39] A. Biswas, K.R. Raslan, Numerical simulation of the modified Korteweg-de Vries equation, Phys. Wave Phenom. 19 (2011) 142–147, https://doi.org/10.3103/S1541308X11020105.
[40] T. Ak, S.B.G. Karakoc, A. Biswas, A new approach for numerical solution of modified Korteweg-de Vries equation, Iran J. Sci. Technol. Trans. Sci. 41 (2017) 1109–1121, https://doi.org/10.1007/s40995-017-0238-5.
[41] T. Ak, S.B.G. Karakoc, A. Biswas, Application of petrov-galerkin finite element method to shallow water waves model: modified Korteweg-de Vries equation, Scientia Iranica B 24 (2017) 1148–1159, https://doi.org/10.24200/SCI.2017.4096.
[42] S.B.G. Karakoc, A quartic subdomain finite element method for the modified KdV equation, Stat., Optim. Inf. Comput. 6 (2018) 609–618, https://doi.org/10.19139/soic.v6i4.485.
[43] S.B.G. Karakoc, Numerical solutions of the mKdV equation via collocation finite element method, Anadolu Univ. J. Sci. Technol. B- Theorit. Sci. 6 (2018) 1–13, https://doi.org/10.20290/aubtdb.420247.
[44] A. Saha, J. Tamang, Effect of q-nonextensive hot electrons on bifurcations of nonlinear and supernonlinear ion-acoustic periodic waves, Adv. Space Res. 63 (2019) 1596–1606, https://doi.org/10.1016/j.asr.2018.11.010.
[45] P.K. Prasad, S. Sarkar, A. Saha, K.K. Mondal, Bifurcation analysis of ion-acoustic superperiodic waves in dense plasmas, Braz. J. Phys. 49 (2019) 698–704, https://doi.org/10.1007/s13538-019-00697-y.
[46] A. Saha, P.K. Prasad, S. Banerjee, Bifurcation of ion-acoustic superperiodic waves in auroral zone of earth's magnetosphere, Astrophys. Space Sci. 364 (2019) 1–6, https://doi.org/10.1007/s10509-019-3671-4.
[47] J. Tamang, A. Saha, Bifurcations of small-amplitude supernonlinear waves of the mKdV and modified Gardner equations in a three-component electron-ion plasma, Phys. Plasmas 27 (2020), https://doi.org/10.1063/1.5115821.
[48] A. Saha, Bifurcation analysis of the propagation of femtosecond pulses for the Triki-Biswas equation in monomode optical fibers, Int. J. Mod. Phys. B 33 (2019), https://doi.org/10.1142/S0217979219503466.
[49] H. Natiq, M.R.M. Said, M.R.K. Ariffin, S. He, L. Rondoni, S. Banerjee, Self-excited and hidden attractors in a novel chaotic system with complicated multistability, Eur. Phys. J. Plus 133 (2018) 1–12, https://doi.org/10.1140/epjp/i2018-12360-y.
[50] S. He, S. Banerjee, K. Sun, Complex dynamics and multiple coexisting attractors in a fractional-order microscopic chemical system, Eur. Phys. J. Spec. Top. 228 (2019) 195–207, https://doi.org/10.1140/epjst/e2019-800166-y.
[51] A. Saha, B. Pradhan, S. Banerjee, Multistability and dynamical properties of ion-acoustic wave for the nonlinear Schrödinger equation in an electron-ion quantum plasma, Phys. Scr. 95 (2020), https://doi.org/10.1088/1402-4896/ab7052.
[52] P.M. Prenter, Splines and Variational Methods, John Wiley & Sons, New York, NY.USA, 1975.
[53] M. Lakshmanan, S. Rajasekar, Nonlinear Dynamics, Springer-Verlag, Heidelberg, 2003.
[54] A. Saha, Bifurcation of travelling wave solutions for the generalized KP-MEW equations, Commun. Nonlinear Sci. Numer. Simulat. 17 (2012) 3539–3551, https://doi.org/10.1016/j.cnsns.2012.01.005.
[55] A. Saha, Bifurcation, periodic and chaotic motions of the modified equal width burgers (MEW-burgers) equation with external periodic perturbation, Nonlinear Dyn 87 (2017) 2193–2201, https://doi.org/10.1007/s11071-016-3183-5.
[56] J.J. Nieto, A. Tores, A nonlinear biomathematical model for the study of intracranial aneurysms, J. Neurol Sci. 177 (2000) 18–23, https://doi.org/10.1016/S0022-510X(00)00315-4.
[57] J. Guckenheimer, P.J. Holmes, Nonlinear oscillations. Dynamical Systems and Bifurcations of Vector Fields, Springer-Verlag, New York, 1983.

[58] A. Sen, S. Tiwari, S. Mishra, P. Kaw, Nonlinear wave excitations by orbiting charged space debris objects, Adv. Space Res. 56 (2015) 429–435, https://doi.org/10.1016/j.asr.2015.03.021.
[59] L. Mandi, A. Saha, P. Chatterjee, Dynamics of ion-acoustic waves in thomas-fermi plasmas with source term, Adv. Space Res. 64 (2019) 427–435, https://doi.org/10.1016/j.asr.2019.04.028.
[60] H. Zhen, B. Tian, H. Zhong, W. Sun, M. Li, Dynamics of the Zakharov-Kuznetsov-Burgers equations in dusty plasmas, Phys Plasmas 20 (2013), https://doi.org/10.1063/1.4818508.